

Magnetic and transport properties of Ge:Mn granular system

Hongliang Li^{a,b}, Yihong Wu^{a,*}, Tie Liu^{a,b}, Shijie Wang^c, Zaibing Guo^b, Thomas Osipowicz^d

^a Department of Electrical and Computer Engineering, National University of Singapore, 4 Engineering Drive 3, Singapore 117576, Singapore

^b Data Storage Institute, DSI Building, 5 Engineering Drive 1, Singapore 117608, Singapore

^c Institute of Materials Research and Engineering (IMRE), 3 Research Link, Singapore 117602, Singapore

^d Department of Physics, National University of Singapore, Singapore 119260, Singapore

Available online 21 November 2005

Abstract

Ge:Mn granular thin films were fabricated on semi-insulating GaAs(001) substrates by molecular beam epitaxy. Transmission electron microscopy and Raman study showed that the sample has a granular structure consisting of GeMn crystallites in a Ge polycrystalline host matrix. A Curie temperature of ~ 300 K was observed in the magnetization measurement, suggesting that the granules are Mn_5Ge_3 . The granular nature of the material was also revealed clearly in the differential conductance vs. bias voltage curves. The unique conductance versus bias voltage curve suggests that the electrical transport is determined by Schottky barriers at the nanoparticle/host matrix interface. This type of material might be useful for studying spin-injections from metallic magnetic nanostructures to semiconductors.

© 2005 Elsevier B.V. All rights reserved.

Keywords: Diluted magnetic semiconductors (DMSs); Granular systems; Schottky barrier; Localization

1. Introduction

Among the different types of diluted magnetic semiconductors (DMSs) which are being studied recently, the Ge-based group IV system has received much attention because of its simple structure, ease in fabrication and potential integration with conventional Si-based electronic devices. Since the successful fabrication of Mn-doped Ge with a Curie temperature (T_c) of 116 K in 2002 by Y. D. Park et al. [1], intensive studies have been done recently in the Ge-based DMS system, and Curie temperatures of 233, 270, 285 and 350 K in $\text{Fe}_{0.05}\text{Ge}_{0.95}$ [2], $\text{Co}_{0.12}\text{Mn}_{0.03}\text{Ge}_{0.85}$ [3], $\text{Ge}_{0.94}\text{Mn}_{0.06}$ [4] and $\text{Ge}_{0.94}\text{Mn}_{0.04}\text{Fe}_{0.02}$ [5] have been reported by different groups, respectively. The ferromagnetism reported so far generally has two origins: (1) carrier-mediated ferromagnetic coupling between the magnetic impurities and (2) secondary phase induced magnetic clusters. Although the former is a more desirable type of DMSs, we believe that the latter will also be very useful if one can precisely control the size and density of magnetic clusters. In this study, a Ge:Mn granular system with an Mn concentration of $\sim 26\%$ was fabricated and its magnetic and transport properties were studied.

2. Experiment details

The Ge:Mn granular thin films (around 40 nm) were fabricated on GaAs (001) semi-insulating substrate using molecular beam epitaxy with a background pressure of about 10^{-9} Torr. During the growth, germanium was evaporated by an electron beam and manganese was evaporated by a K-cell with a temperature of 1073 K. The deposition rate was ~ 3 nm/min at a substrate temperature of 573 K. During film growth, the substrate holder was rotated continuously to improve the uniformity of the thin film. The structural properties of the sample were characterized by transmission electron microscopy (TEM) and Raman spectroscopy. The magnetizations were measured with a superconducting quantum interference device (SQUID–MPMS) magnetometer in the temperature range of 5–400 K. Conventional dc four-probe techniques were used to measure the electrical transport properties. The manganese composition was determined by Rutherford back-scattering (RBS) spectrometry with an estimated error of 10%.

3. Result and discussion

Films with different Mn compositions have been fabricated. In this study, we focus on samples with high Mn concentra-

* Corresponding author. Tel.: +65 6874 2139; fax: +65 6779 1109.

E-mail address: elewuyh@nus.edu.sg (Y.H. Wu).

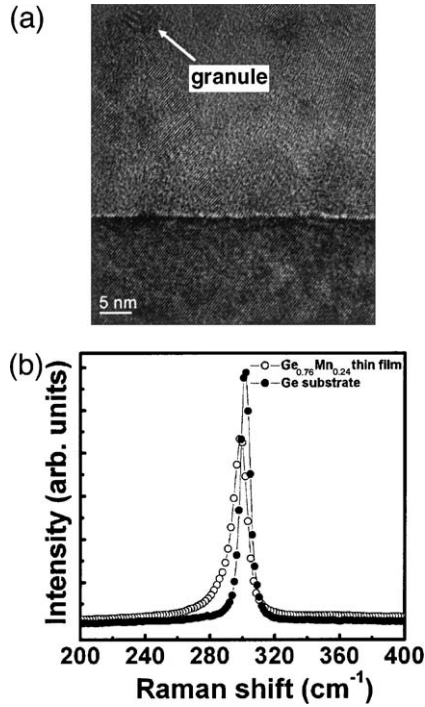


Fig. 1. (a) Bright-field cross-sectional TEM image of $\text{Ge}_{0.76}\text{Mn}_{0.24}$ thin film. The arrow indicates a granule with a diameter of 5 nm. (b) Raman spectra of both the $\text{Ge}_{0.76}\text{Mn}_{0.24}$ thin film and a standard Ge substrate.

tions. Fig. 1(a) shows the bright-field cross-section TEM image of a $\text{Ge}_{0.74}\text{Mn}_{0.26}$ thin film. Different crystalline orientations can be seen clearly in the TEM images, indicating the polycrystalline nature of the thin film. As indicated by the arrow, granules with a diameter of ~ 5 nm embedded in the crystalline matrix can be seen clearly. Although the structure of the clusters can not be determined by the TEM image, as we will discuss shortly, the magnetic property measurement suggested that they are Mn_5Ge_3 . Fig. 1(b) shows the Raman spectra of both the $\text{Ge}_{0.74}\text{Mn}_{0.26}$ thin film and the germanium substrate. The appearance of a strong and sharp peak at about 298 cm^{-1} indicates that the host matrix is polycrystalline Ge. In comparison with single crystalline germanium substrate, a red shift of about 3 cm^{-1} and a low frequency shoulder were observed in the $\text{Ge}_{0.74}\text{Mn}_{0.26}$ thin film. The latter is a typical feature of Ge nanocrystals as discussed in Refs. [5,6]. Although

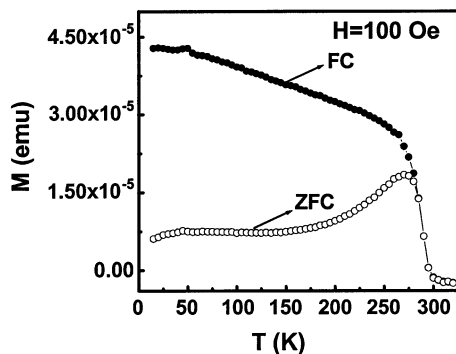


Fig. 2. ZFC and FC curves measured with a magnetic field of 100 Oe in a temperature range of 5 to 320 K.

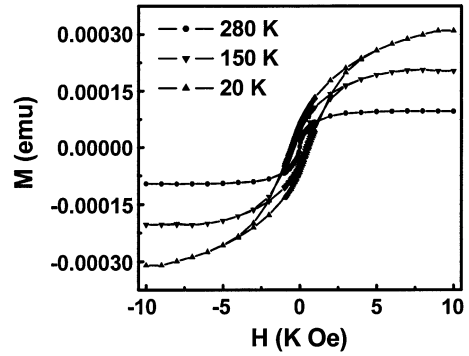


Fig. 3. Field-dependent magnetization curves measured at 20, 150 and 280 K, respectively.

the Mn composition in our sample is higher than that of the epitaxial growth films reported in literature ($< 6\%$), the sample still maintains the germanium microcrystalline structure.

Fig. 2 shows the temperature-dependent magnetization of both zero-field cooled (ZFC) and field-cooled (FC) curves in the temperature range of 5 to 320 K. The sample exhibits a ferromagnetic ordering temperature of approximately 300 K. The separation between ZFC and FC is observed at 285 K. According to the previous reports, both $\text{Mn}_{11}\text{Ge}_8$ and Mn_5Ge_3 exhibit near and above room temperature ferromagnetic properties [7,8]. However, the magnetization of $\text{Mn}_{11}\text{Ge}_8$ exhibits a dramatic drop below 150 K due to antiferromagnetic ordering [7]. Thus, the granules in this system should be Mn_5Ge_3 . The hysteresis loops were measured at different temperatures with a maximum magnetic field of 10000 Oe (Fig. 3). Clear hysteresis has been observed up to 280 K. The slow saturation at low temperatures and small squareness ($M_r = 0.21M_s$ at 20 K) of the curves provide further evidence that the ferromagnetism originates from magnetic granules.

Fig. 4 shows the resistance as a function of temperature. As can be seen from the figure, the resistance increases with decreasing the temperature, which is a typical semiconducting behavior. The rate of resistance change can be divided into two regions: (I) $5 \text{ K} < T < 100 \text{ K}$ and (II) $100 \text{ K} < T < 300 \text{ K}$. Compared to region (I), the resistance increases more rapidly with the decrease of temperature in region (II). As was reported in Ref. [8], Mn_5Ge_3 epitaxial thin film shows a metallic behavior and the resistivity ratio $\rho(300 \text{ K})/\rho(4 \text{ K})$ is ~ 12 .

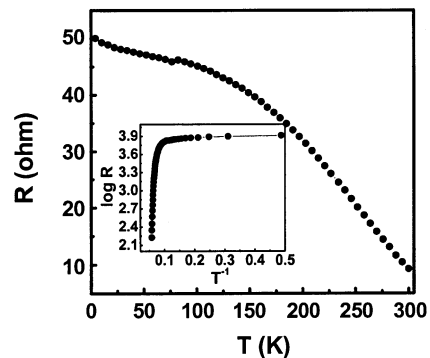


Fig. 4. Temperature-dependent resistance in the temperature range of 5–300 K. Inset: the plot of $\log R$ vs. T^{-1} .

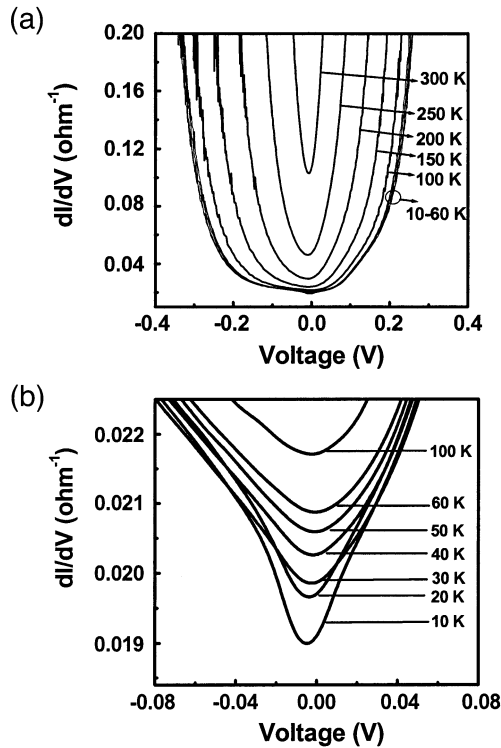


Fig. 5. (a) Conductance–voltage curves at different temperatures; (b) Enlarged portion near the zero-bias region below 100 K.

Thus, the competition between the metallic granules and the semiconductor matrix may result in a slow change of resistance below 100 K. The inset of Fig. 4 shows the plot of $\log R$ vs. T^{-1} . Clearly, the temperature-dependent resistance can be well fitted with an Arrhenius function $\rho = \rho_0 \exp(E_a/kT)$ where E_a is the activation energy, suggesting that the transport is dominated by a thermal activation mechanism. The thermally activated process can be seen even more clearly in the differential conductance versus bias voltage curves (Fig. 5) at different temperatures. The nonlinear I – V curves and corresponding asymmetry between the forward and reverse bias curves are observed at all measurement temperatures. In the high temperature range, the conductance increases sharply with the increase of bias. The curves become broader when the temperature decreases. A flat region appears at low bias voltages when the temperature is below 100 K, suggesting the existence of a Schottky barrier at the nanoparticles/host matrix interface. The enlarged portion near the zero-bias region at low

temperatures is shown in Fig. 5(b). A sharp dip near zero-bias appears below 30 K. The dip becomes less pronounced when temperature increases and disappears above 30 K. Different causes of the conductance dip have been discussed before [9,10], which include localization in amorphous materials or ultrathin film, tunneling through an intermediate state, and magnetic scattering in the electrodes or in the barrier. In our case, charge localization resulting from the disordered granular system may be the cause of the anomaly observed. In order to observe spin-injection effect, we are currently trying to make nanostructures based on these films and then study their transport properties under an external magnetic field.

4. Conclusion

Ge:Mn granular films with a Mn composition of 26% have been fabricated and studied. The film exhibited a Curie temperature of ~ 300 K and a semiconductor-like conduction behavior. Detailed structural, magnetic and electrical transport studies revealed that the film consists of a polycrystalline Ge host matrix embedded with magnetic clusters. This type of material may serve as an ideal system for studying spin-injection between ferromagnets and semiconductors.

References

- [1] Y.D. Park, A.T. Hanbicki, S.C. Erwin, C.S. Hellberg, J.M. Sullivan, J.E. Mattson, T.F. Ambrose, A. Wilson, G. Spanos, B.T. Jopner, *Science* 295 (2002) 651.
- [2] Sungyoul Choi, Soon Cheol Hong, Sunglae Cho, Yunki Kim, John B. Ketterson, Chi-Un Jung, K. Rhie, Bong-Jun Kim, Y.C. Kim, *J. Appl. Phys.* 93 (2003) 7670.
- [3] F. Tsui, L. He, L. Ma, A. Tkachuk, Y.S. Chu, K. Nakajima, T. Chikyow, *Phys. Rev. Lett.* 91 (2003) 177203.
- [4] H. Braak, R.R. Gareev, D.E. Bürgler, R. Schreiber, P. Grünberg, C.M. Schneider, *J. Magn. Magn. Mater.* 286 (2005) 46.
- [5] L. Liu, Z.X. Shen, K.L. Teo, A.V. Kolobov, Y. Maeda, *J. Appl. Phys.* 93 (2003) 9392.
- [6] K.L. Teo, S.H. Kwok, P.Y. Yu, S. Guha, *Phys. Rev., B* 62 (2000) 1584.
- [7] Yamada, K. Maeda, Y. Usami, T. Ohoyama, *J. Phys. Soc. Jpn.* 55 (1986) 3721.
- [8] Changgan Zeng, S.C. Erwin, L.C. Feldman, A.P. Li, R. Jin, Y. Song, J.R. Thompson, H.H. Weitering, *Appl. Phys. Lett.* 83 (2003) 5002.
- [9] E.L. Wolf, *Principles of Electron Tunneling Spectroscopy*, Oxford University Press, New York, 1985.
- [10] J.S. Moodera, Lisa R. Kinder, Terrilyn M. Wong, R. Meservey, *Phys. Rev. Lett.* 74 (1995) 3273.